Accepted for publication in "Combustion Science and Technology"

SPECTROSCOPIC STUDIES OF LOW PRESSURE OPPOSED FLOW METHANE/AIR FLAMES INHIBITED BY $Fe(CO)_5$, CF_3Br, OR N_2

R.R. Skaggs*, K.L. McNesby, R.G. Daniel, B. Homan, and A.W. Miziolek

U.S. Army Research Laboratory

Aberdeen Proving Ground, MD 21005

rskaggs@arl.mil

Abstract

Hydroxyl radical (OH) is measured using laser induced fluorescence in reduced pressure, non-premixed, opposed flow CH_4/air flames inhibited by either N_2, CF_3Br, or $Fe(CO)_5$. Emission spectroscopy is used to qualitatively monitor OH for each inhibited flame as well as to characterize the structure of a $Fe(CO)_5$ inhibited flame. For the flames to which CF_3Br and $Fe(CO)_5$ are added, the OH population decreases approximately proportional to the amount of inhibitor agent added. OH populations decrease faster for flames inhibited by $Fe(CO)_5$ than for flames inhibited by CF_3Br.

Introduction

Fires that occur in non-traditional environments such as aboard combat vehicles, inside aircraft hangers or on board the space shuttle are usually extinguished using halon 1301 (CF_3Br) or halon 1211 (CF_2ClBr). These halogenated hydrocarbons have been implicated as contributing to stratospheric ozone destruction (Montreal Protocol, 1992). In compliance with international agreement, production of halon 1301 and halon 1211 has ceased and current research is focused on finding alternative fire suppressant agents as the current stockpiles of halons are being depleted. The status of halon replacement research has been summarized recently (Miziolek and

Tsang, 1995). The initial search for halon substitutes has concentrated on near chemical relatives of halon 1301 namely hydrofluorocarbons (HFCs) and perfluorocarbons (PFCs). However these compounds have been found deficient in terms of increased weight and volume requirements for fighting the most difficult military fires.

Besides these halogenated hydrocarbons, there are several chemicals, such as iron pentacarbonyl ($Fe(CO)_5$), that are very effective flame inhibitors (Babushok and Tsang, 1997). In fact, $Fe(CO)_5$ may be one of the most effective inhibiting agents ever discovered (Jost et al. 1961; Lask and Wagner, 1962; Bonne et al., 1962; Pitts et al., 1990; Reinelt et al., 1996; Brabson et al., 1996;), but the agent cannot be used in spaces occupied by personnel because it is highly toxic (Pitts et al., 1990). Even though $Fe(CO)_5$ cannot be considered as a viable replacement for halons, understanding the mechanism that is responsible for its superior inhibition effectiveness might provide a path to identifying new inhibitor behavior and therefore new fire suppressant agents.

Background

Flame inhibition by $Fe(CO)_5$ is assumed to proceed by a gas phase mechanism at low inhibitor concentrations (homogeneous) or a gas-solid (heterogeneous) mechanism at high inhibitor concentrations (Jost et al. 1961, Bonne et al., 1962). Specifically, Jost et al. (1961) observed for low pressure, flat, premixed CH_4/air and CH_4/O_2 flames to which small amounts of $Fe(CO)_5$ were added, burning velocities decreased proportionally to the added $Fe(CO)_5$ concentration. The CH_4/O_2 flames were more difficult to inhibit than the CH_4/air and hydrocarbon/air flames as well as $Fe(CO)_5$ inhibition effectiveness decreased at pressures below 1 atmosphere. As $Fe(CO)_5$ concentrations were increased in both flame systems, the relative

inhibition effectiveness appeared to diminish. Lask and Wagner (1962) noted that $Fe(CO)_5$ is less effective at inhibiting H_2 flames than hydrocarbon flames. Further, the use of oxygen rather than air as the oxidizer as well as pressure reductions decreased the relative effectiveness of $Fe(CO)_5$ as an inhibitior. Jost et al. (1961) state that OH radicals are vital to flame propagation chemistry hence OH absorption intensities were measured (Bonne et al., 1962) in the flames. Bonne et al., (1962) did not observe significant differences in the maximum OH concentrations with increasing $Fe(CO)_5$ concentrations for a low pressure, premixed CH_4/air flame but did detect the position of the OH maximum shifted away from the burner surface. Jost et al. (1961) concluded that $Fe(CO)_5$ inhibition occurred because OH was deactivated with the observation of a "delay reaction of the first order in the hydroxyl radical concentration occurred with $Fe(CO)_5$."

More recent investigations (Reinelt and Linteris, 1996, Reinelt et al., 1996) of premixed and non-premixed CH_4/air flames containing $Fe(CO)_5$ have been conducted. For the premixed flames, burning velocity measurements have shown at low $Fe(CO)_5$ concentrations burning velocity reductions are dependent on inhibitor concentrations, but at higher mole fractions the burning velocities were practically independent of the inhibitor mole fraction. The counterflow flame studies indicate that for air side addition of $Fe(CO)_5$ to the flame, the rate of decrease for the extinction strain rate declined as inhibitor concentrations increased. Numerical modeling (Rumminger et al., 1998) of both flame systems demonstrated similar results to the previously cited experiments, which led to the conclusion that inhibition by $Fe(CO)_5$ occurs primarily as a result of H atom removal from the flame by a homogeneous mechanism involving iron containing scavenging species (Reinelt and Linteris, 1996; Reinelt et al., 1996). The authors also indicate that above a certain inhibitor concentration ($\approx$ 100 ppm), a decrease in inhibition occurs due to

condensation of active gas phase species to relatively inactive particles. The cited numerical study suggests a homogeneous mechanism for $Fe(CO)_5$ flame inhibition which is based on the work of Jensen and Jones (1974), who developed a catalytic kinetic mechanism for H atom recombination by iron containing species in the products of rich hydrogen/oxygen/nitrogen flames. The Rumminger et al. (1998) $Fe(CO)_5$ inhibition mechanism indicates that gas phase metal-oxygen monomers ($Fe(OH)_2$, FeOH, and FeO) are formed when $Fe(CO)_5$ is introduced into the flame and they are reaction participants in a catalytic free radical removal mechanisms for H which causes flame inhibition. Rumminger et al. (1998) concluded in their work that after the addition of $\approx$ 100-200 ppm of $Fe(CO)_5$, flame inhibition effectiveness decreases with increasing $Fe(CO)_5$ concentrations because the rate of the homogeneous inhibition reaction is limited by the saturated vapor pressure of iron-containing compounds in the gas phase.

There exists some experimental evidence that in $Fe(CO)_5$ inhibited flames non-gas phase iron-containing particles form. Lask and Wagner (1962) observed that $Fe(CO)_5$ inhibited flames left a deposit and concluded that in the burned flame gases extremely small particles are present that may influence the flame's reaction zone. Kaufman (1958) observed that in the presence of O atoms, $Fe(CO)_5$ produced fine oxide particles that deposited onto the walls of a reaction tube. Bonne et al. (1962) measured the emission intensity and absorption of Fe and FeO at various heights for $Fe(CO)_5$ addition to low pressure CH_4/air and CH_4/O_2 flames. Reinelt and Linteris (1996) observed when $Fe(CO)_5$ is added to the oxidizer stream of a counterflow CH_4/air flame, the original blue flame became a very bright orange color which was attributed to FeO emission near 591 nm. A "rusty" particle deposit was also observed in the exhaust stream after the experiments with $Fe(CO)_5$. The observation of particle formation inside and outside a flame with

iron containing species implies that a heterogeneous reaction may contribute to the inhibition effect of $Fe(CO)_5$.

To date there have been no laboratory measurements of the change in the concentration of radical species with increasing addition of $Fe(CO)_5$ to non-premixed flames. In fact, only limited measurements of radical species in non-premixed flames inhibited by CF_3Br exist (Niioka 1983; Masri et al. 1996; Smyth and Everest, 1996). Presented here are results from studies of the influence that $Fe(CO)_5$, CF_3Br, and N_2 have on the structure of a low pressure, opposed flow, CH_4/air flame. The OH radical profiles have been measured along with their dependencies on inhibitor concentrations as extinction is approached in a reduced pressure, non-premixed, opposed flow, CH_4/air flame inhibited by N_2, CF_3Br, or $Fe(CO)_5$. A low pressure opposed flow flame offers an ideal environment for measurements of flame intermediate species because the flame zone is expanded. For flames inhibited by CF_3Br and $Fe(CO)_5$, the primary mechanism for chemical fire inhibition is due to catalyzing H-atom recombination which in turn reduces the overall available radical pool (H, O, OH) and thus the rate of chain-branching reactions (Westbrook, 1980;1982;1983; Dixon-Lewis and Simpson, 1976). OH was monitored because it is relatively simple to measure and it is a general indicator of the overall radical pool concentration, even though H, O, and OH have been found to not be fully equilibrated in diffusion flames (Smyth et al., 1990). The flames are primarily studied as they approach extinction using OH laser induced fluorescence (LIF) spectroscopy.

Experimental

Apparatus

Figure 1 presents a schematic diagram of the experimental arrangement. The opposed flow burner apparatus is contained within a 200 L combustion chamber. The combustion chamber is a six armed stainless steel cross with the four horizontal arms being 25.4 cm in diameter and the two vertical arms being 30.48 cm in diameter. The opposed jet ducts are mounted in the vertical arms with each head having two axis of motion under computer control. The opposed jet duct diameters are 7.68 cm and the active burner area is approximately 7.6 cm in diameter. Laminar flow is established in the jet ducts with the initial gases impinging on a 0.32 cm thick, porous, stainless steel, sintered disk. The gases flow through a 2.54 cm region before passing through a second, 0.32 cm thick, porous, stainless steel, sintered disk. The second porous disk opens to the combustion chamber. Schlieren images of the gases have shown laminar flow from both ducts. The gases and cooling water are fed to the burner ducts via stainless tubing.

Optical access to the chamber is provided on the four vertical arms of the chamber where 10.16 cm diameter windows are mounted. There are also four additional ports in the horizontal plane, each located between two of the window arms. These ports serve as access for pressure monitoring, thermocouple manipulation, and electrical connections. Also mounted on top and bottom of each window arm are vacuum ports to remove the combustion gases. These eight ports are joined to a single 5.08 cm I.D. tube which feeds the gas to a scrubber mounted on a high volume vacuum pump. The scrubbed exhaust gases are then vented to the atmosphere. All flames were studied at a pressure of 50 torr, the oxidizer flow consisted of 10 L/min synthetic air (79% N_2 + 21% O_2, Matheson UHP Grade) flowing from the upper duct, and the fuel flow was 10 L/min of methane (Matheson UHP Grade) flowing from the lower duct. The gases are regulated

and monitored by a gas handling manifold system constructed from a series of flow controllers (Tylan General). The oxidizer and fuel ducts are separated 3.8 cm. For the flow conditions and flow duct separation, the luminous flame zone is located on the oxidizer side of the stagnation plane and the global strain rate was calculated to be 50.2 sec^{-1} (Seshadri and Williams, 1978). For all studies presented here, the inhibitor agents are added to the oxidizer flow for delivery to the flame zone.

$Fe(CO)_5$ is a liquid at room temperature and its introduction into the flame is accomplished by bubbling argon (Ar) through a flask containing 25 ml of $Fe(CO)_5$ that is immersed in a constant temperature bath maintained at 13 °C. The resulting Ar/ $Fe(CO)_5$ mixture consists of ≈ 2 % $Fe(CO)_5$ and ≈ 98 % Ar. The maximum flow of Ar through the bubbler was 0.41 L/min. At this flow rate, the effect of Ar on the flame is minimal. The gaseous output of the bubbler apparatus passes through a 5 L/min mass flow meter to monitor the Ar/$Fe(CO)_5$ mixture being delivered to the oxidizer stream. The mass flow meter was calibrated for the Ar/$Fe(CO)_5$ mixture using a standard soap bubble technique.

Diagnostics

Flame emission spectra were measured using a Princeton Instruments ICCD camera (Model 120) coupled to a 0.75 m SPEX spectrograph (Model 1702) with a 1200 gr/mm grating controlled by an external Compudrive. A 50 cm focal length lens collects light from the center of the flame and focuses it onto the entrance slits (0.05 mm) of the spectrograph. The determined field of view of this optical arrangement is 1 cm^2. The ICCD camera, which has an active area of

384 x 576 pixels, was operated in a CW manner and each image recorded was acquired with 50 total accumulations on the camera.

Laser induced fluorescence excitation spectra in the flame were measured using a Lambda Physik excimer/dye laser system. The system consists of a Lambda Physik Compex 102 XeCl excimer laser, a Scanmate 2 dye laser (Rhodamine 6g), and a Second Harmonic Generator (SHG). The fundamental output of the dye laser (580 nm wavelength) was frequency doubled in the SHG unit with a BBO crystal to around 290 nm. The UV laser radiation was tuned to the peak of the $P_2(8.5)$ transition at 286.566 nm ((1,0) $A^2\Sigma^+ \leftarrow X^2\Pi$) (Chidsey and Crosley, 1980; Dieke and Croswhite, 1962; Kotlar, 1998). The intensity of this transition is slightly temperature dependent (Eckbreth 1988), varying by approximately 12% over the range of maximum temperatures for the flames studied here. The selected transition varied linearly with input energy. Low laser energies were used and the laser was operated in the linear regime. The UV light output of the SHG unit was focused to the center of the burner chamber using a 50 cm focal length fused silica lens and had a vertical and horizontal beam waist of 0.4 and 0.5 mm, respectively. Fluorescence was collected at 90 degrees to the direction of the excitation laser beam, focused through 0.75 mm horizontal slits to define the collection volume, passed through a band pass filter centered at 312 nm with an 11 nm bandwidth, and detected by photomultiplier tube (PMT) (Phillips Model XP2018B). Fluctuations in laser power were detected by a photodiode that monitored laser induced fluorescence from a cell containing Rhodamine 6g dye.

The output signals from the PMT and monitor photodiode were directed to gated integrator/boxcar averagers (SRS Model SR-250) operating in a 10 shot average mode. The

boxcar gate widths were set to 3 ns. The trigger pulses to the excimer laser and boxcars were supplied by a digital delay pulse generator (SRS Model DG535) at a rate of 10 Hz. Spatially resolved OH LIF profiles are measured by tuning the excitation laser to the peak of the $P_2(8.5)$ transition and, with the beam location fixed, vertically translating the burner assembly.

Results

For the opposed flow CH_4/air flame at a total pressure of 50 torr and a strain rate of 50.2 s^{-1}, **Table I** lists the inhibitor agent concentrations at extinction and the average uncertainties due to measurement variance.

Table 1: Inhibitor concentrations (ppm) and uncertainty (± ppm) at flame extinction

Inhibitor Agent	N_2	CF_3Br	$Fe(CO)_5$
Extinction Concentration	9426	3735	451
Uncertainty	566	672	77

The large degree of variance is believed to be due to changes in the burner cooling. The flow of cooling water to the burner ducts was not monitored precisely and thus the burner performance probably changed slightly from day to day operation. This deficiency is perhaps significant because the burner is operated in a quasiadiabatic condition and thus heat losses from the flame to the burner ducts can cause decreases in extinction concentrations observed experimentally. Preliminary numerical calculations of extinction concentrations for CF_3Br and $Fe(CO)_5$ were 4000 and 271 ppm, respectively (Smooke, 1997). The numerical calculations for both CF_3Br and $Fe(CO)_5$ were performed using kinetic models (Rumminger et al. 1998; Noto et al., 1996). Preliminary numerical calculations by Babushok (1999) using the kinetic model for $Fe(CO)_5$

inhibition of Rumminger et al. (1998) but corrected for the pressure dependence of the FeO + $H_2O \leftrightarrow Fe(OH)_2$ reaction, demonstrated an extinction concentrations of 612 ppm.

It should be noted that addition of N_2 or CF_3Br, to the 50 torr, CH_4/air flame does not significantly alter the visual appearance of the flame, which is a flat, axi-symmetric, blue disk flame. Addition of $Fe(CO)_5$ to the flame causes an orange/yellow luminous zone to appear above the blue luminous zone which is similar to that observed by Reinelt and Linetris (1996). As the $Fe(CO)_5$ inhibited flame approaches extinction, the blue and the orange/yellow luminous zones gradually merge and the flame assumes a uniform bright orange/yellow color. Note: For extinction of all three inhibited flames, the flames appear to extinguish in the flat regions directly between the opposed flow fuel and oxidizer ducts. The orange/yellow luminosity in the $Fe(CO)_5$ inhibited flame is believed to be caused by iron oxide emission (Bonne et al., 1962). The dual flame zone observation, which has been observed in previous $Fe(CO)_5$ studies (Bonne et al., 1962), was further characterized using emission spectroscopy.

For the compositional analysis of the solid particles formed in the flame, particle samples were collected and analyzed using a scanning electron microscope (SEM) and X-ray fluorescence (XRF) techniques. Particle samples were taken from the upper cooled burner duct where large deposits were found and from an uncoated, 0.2 mm diameter Pt/Pt-10 % Rh wire thermocouple inserted into the visible center of a $Fe(CO)_5$ inhibited flame. The collected particulate material appears as a ruddy orange powder. The XRF showed the elemental composition of the particles to be iron and oxygen. An exact ratio of iron to oxygen was not determined, but the SEM analysis

indicated that the size of the particles ranged from 1 to 10 microns, with most being 1 - 2 microns and quasi-spherical in morphology.

Emission Spectroscopy

Emission spectroscopy was used to qualitatively examine the behavior of OH for each inhibited flame as well as the decomposition of $Fe(CO)_5$ upon introduction into the flame. For OH, images were collected from the opposed flow CH_4/air flames seeded with increasing concentrations of N_2, CF_3Br, or $Fe(CO)_5$. Images indicate that for approximately equal inhibitor concentrations added to the flame, the flame to which $Fe(CO)_5$ had been added, demonstrated the smallest OH emission intensity with respect to the flames to which N_2 or CF_3Br had been added. These observations illustrate that addition of $Fe(CO)_5$ to the flame has the greatest effect on the OH population. However further quantification of the results are risky because ground state populations and temperatures calculated from OH emission in flames using a Boltzman distribution can be misleading. That is, nascent OH that is responsible for the chemiluminescence may not be in thermal equilibrium with ground electronic state OH and other combustion gases.

Figure 2 shows a representative emission image collected in the 554 nm wavelength region from the centerline of an opposed flow CH_4/air with 10 % of the experimentally determined extinction concentration of $Fe(CO)_5$ added to the oxidizer flow. The addition of $Fe(CO)_5$ to a low-pressure CH_4/air diffusion flames changes the molecular emission spectra to include iron species such as FeO and FeOH as well as atomic iron lines (Daniel et al., 1997). These modifications to the molecular emission spectra alter the flame's emission intensity which is illustrated in **Figure 2**. The spatial mapping indicates that some of the $Fe(CO)_5$ has decomposed

prior to the luminous flame region at approximately 10.4 ± 1 mm from the oxidizer duct with a majority of the emission in this spectral region attributed to FeO (Gaydon, 1972). The lower continuum, at approximately 14.8 ± 1 mm from the oxidizer duct, is due to the broadband luminosity of the hydrocarbon flame. It should be noted that earlier emission images (Daniel et al., 1997) of CH emission from similar low pressure CH_4/air flames seeded with $Fe(CO)_5$ showed an additional region of emission intensity closer to the oxidizer duct which was not observed in both uninhibited and inhibited flames seeded with N_2 or CF_3Br. The additional intensity was identified as iron lines not present in the uninhibited flame.

The recognition of the formation of iron particles in the flame invokes suggestions of heterogeneous chemistry occurring. Recent work by Babushok et al. (1998), who modeled the effect of an ideal gas-phase flame inhibitor using gas kinetic rate constants for a set of radical scavenging and inhibitor-regenerating reactions, indicate otherwise. Calculations were conducted for a premixed flame containing $Fe(CO)_5$ and a premixed flame with the ideal gas phase flame inhibitor. The calculations showed that the burning velocities, which were very non-linear as inhibitor concentrations increased, for both flame systems were nearly equal for the same inhibitor quantities. From this result the authors concluded that the $Fe(CO)_5$ inhibition mechanism is dominated by homogeneous gas-phase chemistry when the inhibitor is added in small concentrations (Babushok et al. 1998).

Laser Induced Fluorescence

The effectiveness of a particular flame inhibitor is typically characterized by its influence on a flame's propagation chemistry. The most common indicators of the overall reaction rates for

premixed and opposed flow flame systems are the burning velocity and extinction strain rate respectively. For premixed flames, the addition of an inhibitor decreases the burning velocity. For diffusion flames, the addition of an inhibitor increases the characteristic chemical reaction time while the characteristic flow time remains the same. Thus the inhibitor concentration increase causes chemical reactions to slow down relative to the characteristic flow time which eventually can lead to flame extinction. For premixed and non-premixed systems, measurements of radical concentrations (O, H, OH) serve as useful indicators of the chemical rates that are being affected because chemical inhibiting agents act to reduce the superequilibrium concentration of radicals. Radical concentrations reach their maximum concentrations in the flame reaction zone and then decay toward equilibrium values. Thus, if an inhibitor is present, it can reduce the maximum radical concentrations toward equilibrium values and show the amount of chemical inhibition present (Williams and Fleming, 1999). Radical measurements are thus directly related to burning velocity and extinction strain rate measurements.

Figure 3 shows representative OH LIF profiles measured in flames to which $Fe(CO)_5$, CF_3Br, or N_2 were added. The inhibitor concentrations are approximately 50 percent of the concentration required for extinction by N_2, CF_3Br, and $Fe(CO)_5$, respectively. The data shown have been normalized to the peak intensity of the OH LIF profile measured in an uninhibited flame. The profiles in **Figure 3** illustrate that at approximately 50 percent of the inhibitor concentrations required for extinction, the flame to which N_2 has been added has the higher OH LIF maximum intensity followed by the flame to which CF_3Br has been added. The OH LIF measured in the flame to which $Fe(CO)_5$ has been added has the lowest intensity.

Addition of an inhibitor to the flame gives rise to modifications in the flame structure. Specifically, addition of an inhibitor can change the position and width of the flame's reaction zone. First, for the uninhibited flame, the location of the average OH LIF maximum from the oxidizer duct is 14.34 ± 0.05 mm. The addition of N_2 and CF_3Br to the flame slightly shifts the position of the OH LIF maximum toward the oxidizer duct to locations of 13.65 and 14.12 mm respectively. The profile location analysis demonstrates that shifts of the OH maximum position with increasing inhibitor concentrations are relatively small. It is of interest that N_2 addition to the flame results in a larger shift to the oxidizer duct than addition of either CF_3Br or $Fe(CO)_5$. Preliminary numerical calculations, Babushok (1999), using the kinetic model for $Fe(CO)_5$ inhibition of Rumminger et al. (1998) but corrected for the pressure dependence of the FeO + $H_2O \leftrightarrow Fe(OH)_2$ reaction, demonstrated the position of the OH maximum concentration at 13 mm from the oxidizer duct.

Second, previous studies (Peters, 1983; Liew et al., 1984; Haworth et al., 1988; Bilger, 1988; Roberts 1992; Miller, 1996) have shown that a decrease in the flame's reaction zone width indicates increased localized strain, which can cause local quenching or flame extinction. The width of the flame's reaction zone may be characterized by the width of a radical profile (Miller, 1996). For the analysis of the radical profile shape modifications, the profiles were fit to a Gaussian function. The width of the flame zone has been defined here as the distance of one half of the maximum intensity of the Gaussian OH profile, i.e. Full Width Half Maximum (FWHM). The determined OH profile width for the uninhibited flame was 5.67 ± 0.08 mm. Addition of N_2 does not change the profile width. The addition of $Fe(CO)_5$ and CF_3Br narrow the profile widths

to 5.22 and 5.50 mm respectively. Thus, the addition of inhibitor agents has a relatively small influence on the profile width for the low pressure methane flame studied here.

Figure 4 presents normalized OH LIF peak intensities versus inhibitor concentrations. For normalization, the OH maximum intensity from the uninhibited flame was used. The presented data are uncorrected for collisional quenching and temperature dependence and the major source for error in the peak OH LIF intensities is the laser shot-to-shot variation. The shot-to-shot variance occurs as the laser energy is scanned over the spectral region of interest. The shot-to-shot uncertainty averaged ± 1.5 % which contributes to the overall measurement uncertainty of 4 %. The **Figure 4** data show the relative effectiveness of the studied inhibitors: Flames inhibited by $Fe(CO)_5$ and CF_3Br demonstrate decreases in OH populations that are quasi proportional to the inhibitor concentrations. Flames inhibited by N_2 demonstrate non-linear behavior with initially small changes in OH and more rapid decreases as extinction is approached. From **Figure 4**, the final measurable OH data points which are near each flame's extinction point concentration, the normalized maximum intensity of OH is approximately the same for all studied inhibitors 0.73-0.67. Thus, there is approximately a 30 % decrease in the normalized OH intensity at extinction for each inhibitor. It should be noted that preliminary numerical calculations, Babushok (1999), using the kinetic model for $Fe(CO)_5$ inhibition of Rumminger et al. (1998) but corrected for the pressure dependence of the $FeO + H_2O \leftrightarrow Fe(OH)_2$ reaction, demonstrated a normalized OH maximum concentration at extinction of 0.73. The ratio of each inhibitors' concentration relative to CF_3Br near extinction is N_2:CF_3Br:$Fe(CO)_5$ = 2.5:1:0.11 indicating that the $Fe(CO)_5$ flame inhibition effectiveness is approximately a factor of 10 greater than CF_3Br. These results are similar to Reinelt and Linetris (1996) who observed that 500 ppm $Fe(CO)_5$ added to the air

stream of an atmospheric pressure, CH_4/air, counterflow flame reduced the strain by $\approx$ 30 %, while addition of 5000 ppm CF_3Br reduced the strain to approximately 20 %. Thus, $Fe(CO)_5$ is the most effective agent studied here on a concentration basis.

Measurements (Smyth et al., 1996 and Masri et al., 1996) of OH concentrations in non-premixed atmospheric pressure hydrocarbon flames have shown decreasing OH concentrations with increasing CF_3Br concentrations. The observed quasi monotonic decrease of OH radical in the flames studied here with increasing of CF_3Br and $Fe(CO)_5$ concentrations is also similar to decreases of chain carrier concentrations in the reaction zone of simulated premixed C1-C2 flames with CF_3Br, CF_3I, CF_4, C_2F_6, and C_2F_5H additives (Noto, 1996). Uncorrected OH absorption profile measurements by Bonne and co-workers (1962) appear to show a slight decrease in the integrated OH concentrations, i.e. area under curves, with increasing $Fe(CO)_5$ concentrations for the studied low pressure, premixed, stoichiometric methane/air flame (60 torr).

It should be noted that the saturation effect (leveling-off), which was observed for burning velocities in atmospheric pressure, premixed methane flames seeded with $Fe(CO)_5$ (Reinelt and Linteris, 1996; Reinelt et al. 1996; Rumminger, 1998), was not observed in this work. Typically, two types of saturation are discussed in the literature: (1) saturation of chemical influence (Noto et al., 1996), and (2) saturation due to condensation processes (Reinelt and Linteris, 1996). Both processes result in a decrease in inhibitor efficiency with increased inhibitor concentration, but the later is believed to dominate for $Fe(CO)_5$ inhibited flames. The inhibited flames studied here are at low pressure, i.e. less than 0.1 atm. Comparing our results with the study of Bonne et al. (1962) who studied the influence of $Fe(CO)_5$ on the burning velocities of premixed CH_4/O_2 flames from 1

atm. to 0.1 atm demonstrates that there exist some similarities. At 1 atm, addition of 0.03 % $Fe(CO)_5$ to the flame decreased the burning velocity ≈ 7.5 %, while at 0.5 atm addition of 0.03 % $Fe(CO)_5$ decreases the burning velocity ≈ 6 %. In premixed CH_4/air flames, addition of 0.01 % $Fe(CO)_5$ at 1 atm caused the burning velocity to decrease 24 % while at 0.5 atm the decrease in burning velocity was only 8-9 %. Obviously, $Fe(CO)_5$ has a more pronounced effect in the CH_4/air flames, but for both systems the decreases in burning velocities were observed to be linear at all pressure conditions and the inhibitor influence of $Fe(CO)_5$ appears to diminish with decreasing pressure. Note: To date there does not exist any experimental data demonstrating the $Fe(CO)_5$ saturation effect for inhibited opposed flow diffusion flames. Thus, with low inhibitor loadings, low pressures, and a CH_4/air flame being used in our study, the decreases in OH seen for CF_3Br and $Fe(CO)_5$ addition to the flame are due to reduction of the flames OH superequilibrium concentrations. Inhibitor efficiencies observed here are probably pressure dependent and as a result the rates of some of the chemical inhibition reactions are probably pressure dependent.

Conclusions

The experimental results presented here demonstrate chemical and physical changes in flame structure as extinction is approached in a low pressure, non-premixed, CH_4/air flame inhibited by either N_2, CF_3Br, or $Fe(CO)_5$. The following conclusions are drawn from this study:

- A two-zone luminous flame structure for a $Fe(CO)_5$ inhibited flame (blue and orange luminous zones) is observed.
- For the first time, LIF measurements of OH in the reaction zone of a low pressure opposed flow flame have been performed as inhibitor concentrations were increased until flame extinction.

- Decreases in OH levels are observed with increases of $Fe(CO)_5$ and CF_3Br concentrations in the flame.

- The inhibitor efficiencies relative to CF_3Br were 2.5:1:0.11 for N_2:CF_3Br:$Fe(CO)_5$. The approximate factor of 10 difference between the CF_3Br and $Fe(CO)_5$ flames implies that $Fe(CO)_5$ is the most effective agent studied here on a concentration basis.

- Analysis of obtained OH concentrations show that the addition of the studied inhibitors in the low pressure flame has a relatively small effect on the locations of the OH maximum intensities.

- The addition of $Fe(CO)_5$ and CF_3Br slightly narrows the width of the flame reaction zone.

Acknowledgments

The authors would like to thank M.D. Smooke of Yale University for numerical calculations of the inhibited opposed flow flames. Thanks also to E. Lancaster for his help with the experimental arrangements. Much of the OH LIF data analysis was aided through the generous guidance of A. Kotlar. Special thanks to V. Babushok of NIST with insightful suggestions and comments concerning experiments and the manuscript. This research is part of the Department of Defense's Next Generation Fire Suppression Technology Program, funded by the DoD Strategic Environmental Research and Development Program (SERDO). Partial financial support was given by the U.S. Army TACOM (Steve McCormick). Finally R. Skaggs would like to acknowledge financial support from the Army Research Laboratory through an American Society for Engineering Education Postdoctoral Fellowship.

Figures

Figure 1: Schematic diagram of the experimental arrangement.

Figure 2: Representative emission image collected around 554 nm from the centerline of the low pressure, opposed flow, CH_4/air flame with 10 percent of the concentration required to extinguish the flame by $Fe(CO)_5$ added to the oxidizer flow. The air and fuel ducts at the top and the bottom of the image respectively.

Figure 3: LIF OH profiles collected from CH_4/air flames containing 4721 ppm of N_2 (○), 1996 ppm of CF_3Br (Δ), and 229 ppm of $Fe(CO)_5$ (❑). The inhibitor concentrations are 50, 53, and 51 percent of the concentration required for extinguishment by N_2, CF_3Br, and $Fe(CO)_5$, respectively.

Figure 4: Dependence of normalized maximum OH LIF intensity on inhibitor concentration. The lowest experimental measurements of OH intensity correspond to near-extinction conditions. The (○) are the N_2 data, the (Δ) are the CF_3Br data , and the (❑) are the $Fe(CO)_5$ data.

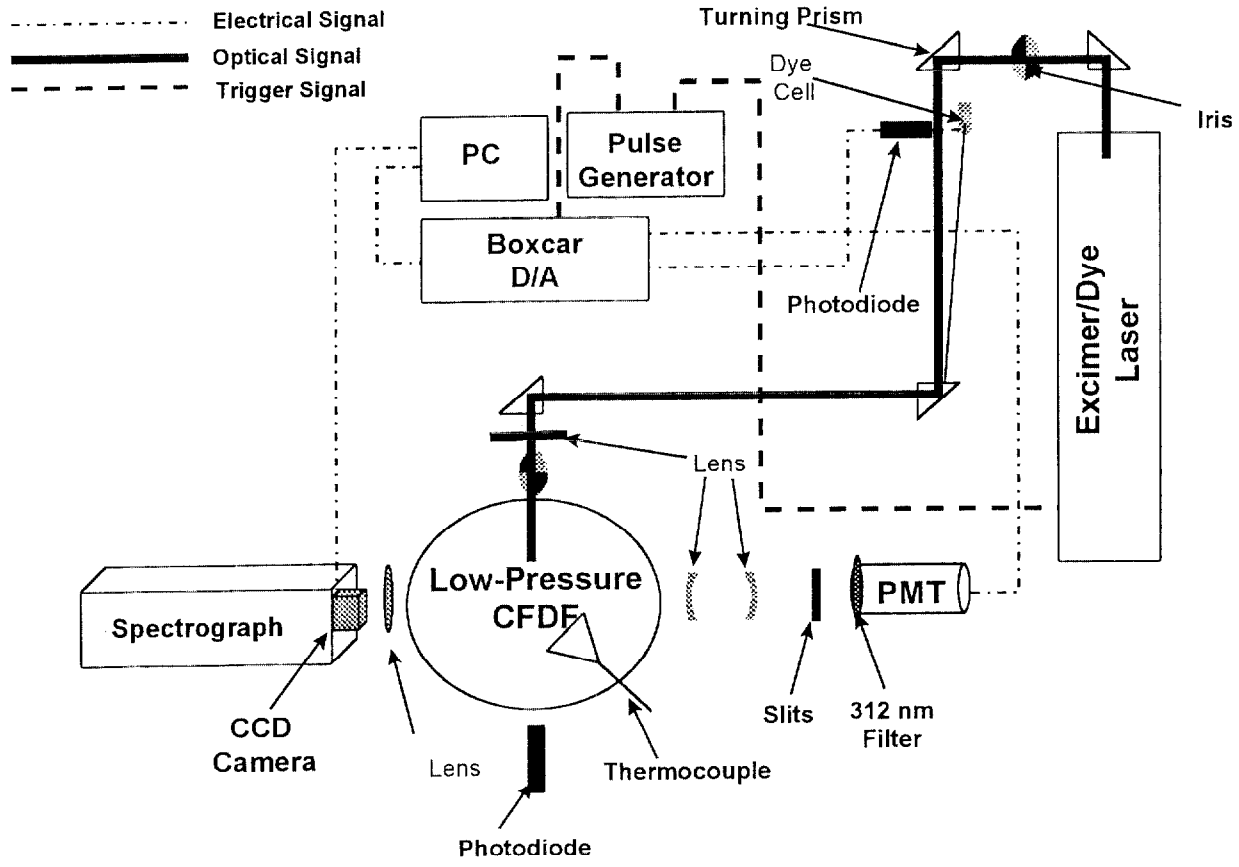
Electrical Signal
Optical Signal
Trigger Signal
Turning Prism
Dye Cell
Iris
PC
Pulse Generator
Boxcar D/A
Photodiode
Excimer/Dye Laser
Lens
Low-Pressure CFDF
Spectrograph
PMT
CCD Camera
Lens
Thermocouple
Slits
312 nm Filter
Photodiode

Figure 1

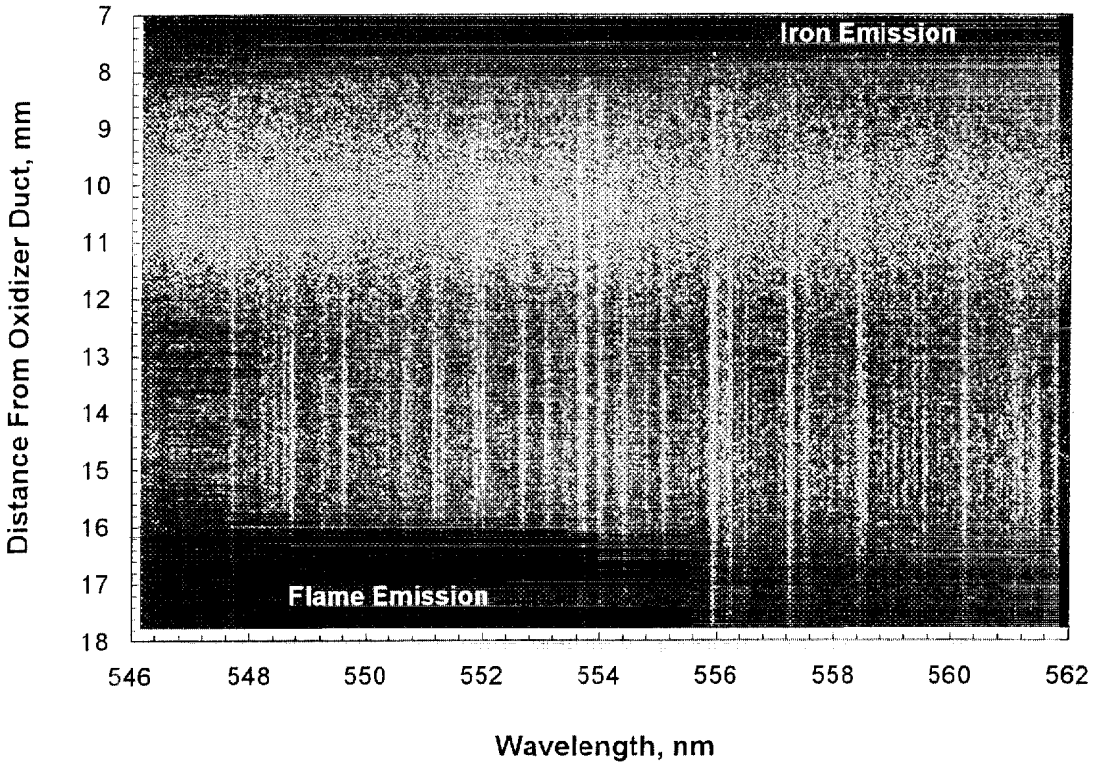
Iron Emission
Flame Emission
Distance From Oxidizer Duct, mm
7
8
9
10
11
12
13
14
15
16
17
18
546
548
550
552
554
556
558
560
562
Wavelength, nm

Figure 2

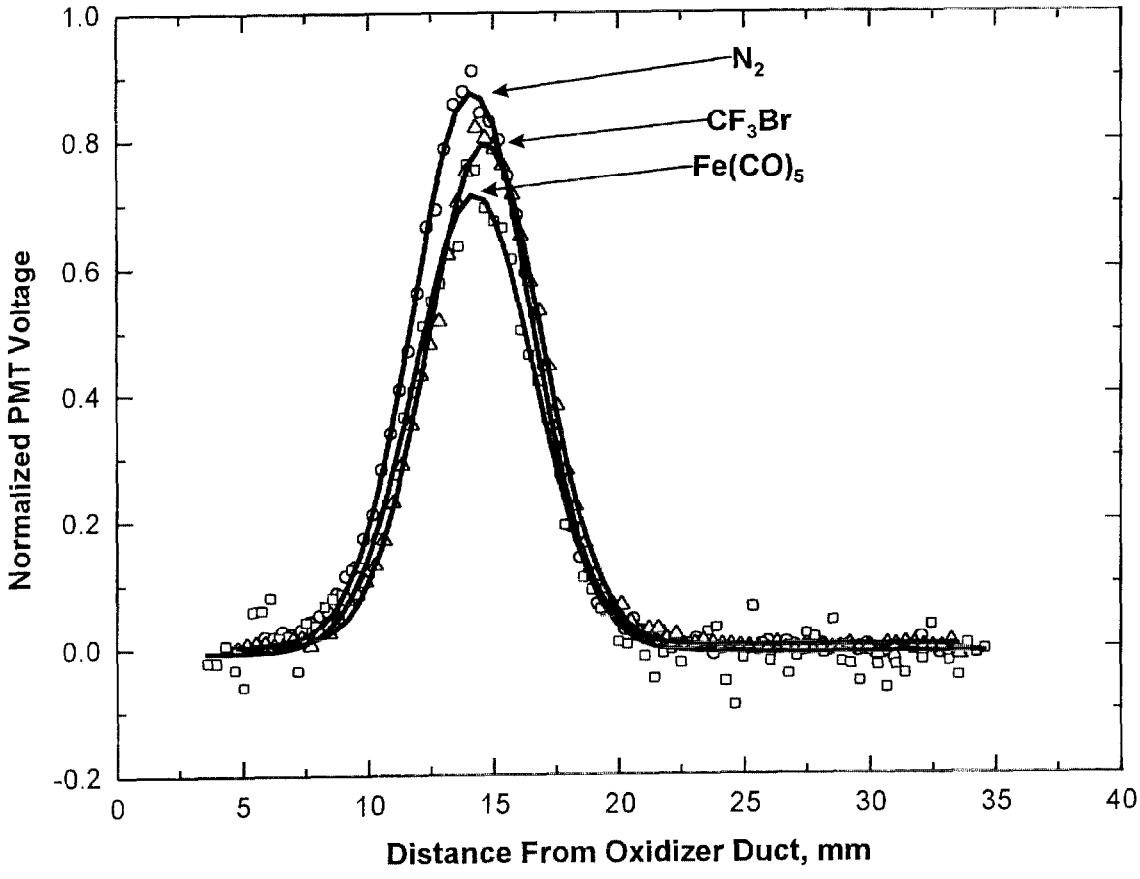
1.0
0.8
0.6
0.4
0.2
0.0
-0.2
0
5
10
15
20
25
30
35
40
Normalized PMT Voltage
Distance From Oxidizer Duct, mm
N_2
CF_3Br
$Fe(CO)_5$

Figure 3

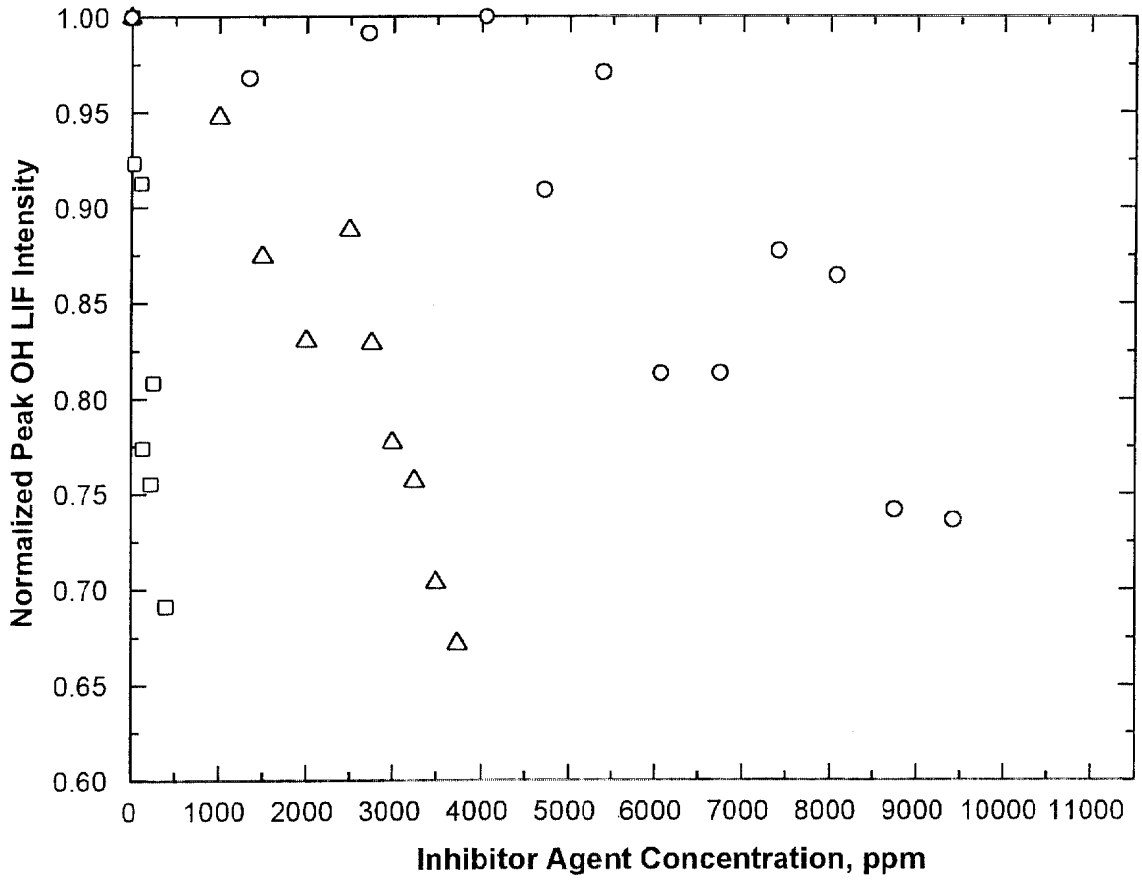
Normalized Peak OH LIF Intensity
1.00
0.95
0.90
0.85
0.80
0.75
0.70
0.65
0.60
0
1000
2000
3000
4000
5000
6000
7000
8000
9000
10000
11000
Inhibitor Agent Concentration, ppm

Figure 4

References

1. Babushok, V., Tsang, W., Linteris, G., Reinelt, D. (1998) Chemical Limits to Flame Inhibition Combustion and Flame, 115,551.
2. Babushok, V. and Tsang, W. (1997) Preliminary Literature Survey of "Superagent" Fire Extinguishing Compound Relative Effectiveness NIST Technical Report, US Department of Commerce.
3. Babushok, V. (1999) Private Communication.
4. Bilger, R.W. (1988) The Structure of Turbulent Non-Premixed Flames Twenty-Second Symposium (International) on Combustion, The Combustion Institute, Pittsburgh, p.1377.
5. Bonne, U., Jost, W., and Wagner, H.G. (1962) Iron Pentcarbonyl in Methane-Oxygen (or Air) Flames Fire Research Abstracts and Reviews 4: 6.
6. Brabson, G.D., Walters, E.A., Schiro, J., Spencer, C., Tapscott, R.E, Patterson, R.A., (1996) Flame Extinguishment by Metal Containing Agents Proceedings of the Halon Options Technical Working Conference, Albuquerque, New Mexico, p.213.
7. Chidsey, I.L., and Crosley, D.R., (1980) Calculated Rotational Transition Probabilities for the A-X System of OH J Quant. Spectrosc. Radiat. Transf, 23, 187.
8. Daniel, R.G., McNesby, K.L., Skaggs, R.R., Sagear, P., and Miziolek, A.W. (1997) Spectroscopy of Inhibited Counterflow Diffusion Flames Proceedings of the 1997 JANNAF Combustion Subcommittee Meeting, West Palm Beach, FL.
9. Dieke, G.H., and Croswhite, H.M., (1962) The Ultraviolet Bands of OH Fundamental Data J Quant. Spectrosc. Radiat. Transf. 2, 97.

10. Dixon-Lewis, G. and Simpson, R.J. (1976) Aspects of Flame Inhibition by Halogen Compounds Sixteenth Symposium (International) on Combustion, The Combustion Institute, Pittsburgh, p.1111.

11. Eckbreth, A.C., (1988). Laser Diagnostics for Combustion Temperatures and Species, Abacus Press, Cambridege Mass.

12. Fourth Meeting of the parties to the Montreal Protocol on Substances that Deplet the Ozone layer, 23-25 Nov 1992, Copenhagen. Doc.no. UNEP/Ozl.Pro.4/15 (Nairobi:UNEP, 1992), 32. The full text of the London and Copenhagen amendments to the Montreal Protocol on Substances that Deplete Ozone layer with the Montreal Protocol attached as an appendix can be found at gopher://gopher.law.cornell.edu/00/foreign/fletcher/MONTREAL-1992.txt.

13. Gaydon, A.G. (1972). The Spectroscopy of Flames second edition, John Wiley and Sons, New York.

14. Haworth, D.C., Drake, M.C., and Blint, R.J., (1988) Stretched Laminar Flamelet Modeling of a Turbulent Jet Diffusion Flame Combust. Sci. Technol. 60, 287.

15. Jensen, D.E., and Jones, G.A. (1974) Catalysis of Radical Recombination in Flames by Iron J. Chem. Phys. 60 (9), 3421-3425.

16. Jost, W., Bonne, U., and Wagner, H.G. (1961) Iron Carbonyl Found to be Powerful Flame Inhibitor Chemical and Engineering News, vol. 39, p. 76.

17. Kaufman, F. (1958). The Air Afterglow and its Use in the Study of Some Reactions of Atomic Oxygen Proc. Roy. Soc. (London) A247, 123.

18. Kotlar, A. (1998). Private Communication.

19. Lask, G., and Wagner, H. Gg. (1962) Influence of Additives on the Velocity of Laminar Flames Eighth Symposium (International) on Combustion, The Combustion Institute, Pittsburgh, Williams and Wilkens, p.432.

20. Liew, S.K., Bray, K.N.C., and Moss, J.B., (1984) A Stretched Laminar Flamelet Model of Turbulent Non-Premixed Combustion Combust. Flame 56, 199.

21. Masri, A.R., Dally, B.B., Barlow, R.S., and Carter, C.D. (1996) The Structure of Laminar Diffusion Flames inhibited with CF_3Br Combust. Sci. Technol. 113-114, 17.

22. Miller, J.H., (1996) "Applications of Conserved Scalars to Combustion Chemistry" Chemical and Physical Processes in Combustion, p.1.

23. Miziolek, A.W. and Tsang, W. (1995) Halon Replacements: Technology and Science, ACS Symposium Series 611, American Chemical Society, Washington, DC.

24. Niioka, T, Mitani, T., and Takahashi, M. (1983) Experimental Study on Inhibited Diffusion and Premixed Flames in a Counterflow System Combust. Flame 50, 89.

25. Noto, T., Babushok, V., Burgess, D.R., Hamins, A., Tsanf, W., Miziolek, A.W. (1996) Effect of Halogenated Flame Inhibitors on C1-C2 Organic Flames" Twenty-Sixth Symposium (International) on Combustion, p.1377.

26. Pitts, W.M., Nyden, M.R., Gann, R.G., Mallard, W. G., and Tsang, W., (1990) Construction of an Exploratory List of Chemicals to Initiate the Search for Halon Alternatives, NIST Technical Note 1279, US Department of Commerce, Chapter 3: Section J., p73.

27. Peters, N. (1983) Local Quenching Due to Flame Stretch and Non-Premixed Turbulent Combustion Combust. Sci. Technol. 30, 1.

28. Reinelt, D., and Linteris, G.T. (1996) "Experimental Study of the Inhibition of Premixed and Diffsuion Flames by Iron Pentacarbonyl" Twenty-Sixth Symposium (International) on Combustion, The Combustion Institute, Pittsburgh, p.1421.

29. Reinelt, D., Linteris, G.T., and Babushok, V. (1996) Numerical Study of the Inhibition of Premixed and Diffusion Flames by Iron Pentcarbonyl Chemical and Physical Processes in Combustion, p. 273.

30. Roberts, Wm. L., Driscoll, J.F., Drake, M.C., and Ratcliffe, J.W. (1992) OH Fluorescence Images of The Quenching of a Premixed Flame During an Interaction with a Vortex Twenty-Fourth Symposium (International) on Combustion, The Combustion Institute, Pittsburgh, p.169.

31. Rumminger, M.D., Reinelt, D., Babushok, V.I., and Linteris, G.T. (1998) Numerical Study of the Inhibition of Premixed and Diffusion Flames by Iron Pentacarbonyl Combust. Flame 116, 207.

32. Seshadri, K. and Williams, F. (1978) Laminar Flow Between Parallel Plates with Injection of a Reactant at High Reynolds Numbers Int. J. Heat and Mass Transfer 21, 251.

33. Smooke, M.D. (1997). Private Communication.

34. Smyth, K.C., and Everest, D. (1996) The Effect of CF_3I Compared to CF_3Br on OH and Soot Concentrations in Co-Flowing Propane/Air Diffusion Flames Twenty-Sixth Symposium (International) on Combustion, The Combustion Institute, Pittsburgh, p.1385.

35. Smyth, K.C., Tjossem, P.J.H., Hamins, A., and Miller, J.H. (1990) Concentration Measurments of OH and Equilibrium Analysis in a Laminar Methane-Air Diffusion Flame Combust. Flame 79, 366.

36. Westbrook, C.K. (1980) Inhibition of Laminar Methane-Air and Methanol-Air Flames by Hydrogen Bromide Combust. Sci. Technol. 23, 191.

37. Westbrook, C.K. (1982) Inhibition of Hydrocarbon Oxidation in Laminar Flames and Detonations by Halogenated Compounds Nineteenth Symposium (International) on Combustion, The Combustion Institute, Pittsburgh, p. 127.

38. Westbrook, C.K. (1983) Numerical Modeling of Flame Inhibition by CF_3Br Combust. Sci. Technol. 34, 201.

39. Williams, B.A. and Fleming, J.W. (1999) Suppression Mechanisms of Alkali Metal Compounds, Proceedings of the Halon Options Technical Working Conference, Albuquerque, New Mexico, in press.